WSRC-MS-99-00204

February 9, 1999

KEYWORDS
Plutonium metal
Experiments
Lattices

RETENTION:
LIFETIME

Experiments of Water-Moderated Plutonium Metal Arrays
Part II - Analysis

Michelle Pitts and Farzad Rahnema
Nuclear Engineering and Health Physics Programs
George W. Woodruff School of Mechanical Engineering
Georgia Institute of Technology
Atlanta, Georgia 30332-0405

T. G. Williamson and Fitz Trumble
Westinghouse Safety Management Solutions
1993 S. Centennial Drive
Aiken, SC 29803

Prepared for Publication in Nuclear Science and Engineering

Experiments of Water-Moderated Plutonium Metal Arrays
Part II - Analysis

Michelle Pitts and Farzad Rahnema
Nuclear Engineering and Health Physics Programs
George W. Woodruff School of Mechanical Engineering
Georgia Institute of Technology
Atlanta, Georgia 30332-0405

T. G. Williamson and Fitz Trumble
Westinghouse Safety Management Solutions
1993 S. Centennial Drive
Aiken, SC 29803

This document was prepared in conjunction with work accomplished under Contract No. DE-AC09-96SR18500 with the U. S. Department of Energy.

Abstract

As part of the International Criticality Benchmark Evaluation Project, 26 experiments are analyzed for use as benchmark experiments for validation of computer codes and cross sections. The experiments consisted of water-moderated plutonium metal arrays of size 2x2xN, where N =2-5 or 3x3x3. Of the 26 experiments, 22 were chosen to develop benchmark models which are described in detail, including

geometry and material data. A sensitivity study was performed to determine the uncertainty on the k_{eff} value due to measurement uncertainties or limits of accuracies. For all benchmark models, k_{eff} values were found using MCNP with continuous-energy ENDF/B-V cross sections, MCNP with continuous energy ENDF/B-VI cross sections, and KENO-V.a with 27-group ENDF/B-IV cross sections. For one case, the codes overestimated k_{eff} by more than 1%. The experiments were grouped for three parameters: plutonium mass, horizontal spacing, and vertical spacing. For each parameter, a bias value was found. In all cases, MCNP with ENDF/B-VI cross sections had the smallest difference in the average k_{eff}. This same result was found when all experiments were grouped together. However, if the one experiment that was significantly overestimated was excluded, the smallest difference in the average k_{eff} was found for KENO-V.a with ENDF/B-IV cross sections.

I. Introduction

In Part I of this paper, 33 critical experiments were described in detail. These experiments were performed at the Rocky Flats Critical Mass Laboratory. The first set of experiments, which listed 23 experimental configurations with critical water heights, began in late 1973 and ended in early 1976. Fifteen additional critical configurations were reported in reference 1. However, these configurations were not actual experiments. Instead, the vertical spacing was derived from fully reflected subcritical experiments. These configurations are not evaluated in this paper. For the second set of experiments, 10 critical configurations were reported. These experiments began in May of 1982 and ended in January 1983.

Although the plutonium metal cylinders were the same for both sets of experiments, the support structure and tank in which the experiments were performed differed. The first program used trays to hold the plutonium while the second program utilized long aluminum sleeves. In addition, the experiments of the first set were performed in an aluminum right circular cylinder tank. The second program used a square plastic-walled tank.

As part of the International Criticality Safety Benchmark Evaluation Project (ICSBEP), these experiments were evaluated for use by nuclear criticality specialists in validating computer codes and cross sections.[2,3] This paper will form benchmark descriptions of the experiments, including geometry and material data. In addition, k_{eff} values using the benchmark models will be found for two computer codes and three cross section libraries, namely MCNP[4] with continuous energy ENDF/B-V[5] and ENDF/B-VI[6] cross section data and KENO-V.a[7] with 27-group ENDF/B-IV cross sections.

Evaluation of experiments includes three main activities: description of the experimental configuration, sensitivity analysis, and description of a benchmark model. Since the experiments to be evaluated here were described fully in Part I, only the sensitivity analysis and the benchmark model will be given in this paper. Details necessary for the analysis will be provided where appropriate. The sensitivity analysis determines the effect on k_{eff} due to any limits of accuracy or uncertainty in the experimental description and is found in Section II. Description of a benchmark model includes a simplified geometry description, relevant material data, and k_{eff} values. Section III provides the benchmark models for the two sets of experiments. K_{eff} values found using the benchmark model are given and discussed in Section IV. Section V provides some concluding remarks.

Results for experiments that were reported with a critical water height were given in Tables 6 and 7 of Part I. Seven experiments reported with large uncertainties in critical water height (> 5 mm) are not considered acceptable as benchmark experiments and, therefore, are also not included in this evaluation. In addition, the results of one of these seven experiments (Exp. 22 of Table 6 in Part I) were questionable since this configuration lay between two subcritical configurations. This measurement is not considered valid for benchmarking purposes. Table 1 shows the critical data for the 26 measurements that are evaluated in this analysis. These experiments have been renumbered for ease of reference.

Table 1. Experimental Critical Configurations

Case Number	Experiment Number	Horizontal Spacing (mm)[a] $\Delta X = \Delta Y$	Vertical Spacing ΔZ (mm)[a]	Between Trays (mm)	Height of Top of Top Tray (mm)	Water Height (mm) [b]
Array Size: 2 x 2 x 2 (24,231 g Pu)						
1	13	76	133.4	50.8	316.0	202 ± 0.5
2	14	76	184.2	101.6	366.8	235 ± 1
3	21	76	214.6	132.1	397.2	246 ± 2
4	19	76	235.0	152.4	417.6	463 ± 3
5	30	90	108.0	25.4	290.6	235.5 ±0.5
6	31	90	133.4	50.8	316.0	308.8 ± 0.5
7	6	100	100.6	18.03	283.2	263 ± 1
8	8	100	126.0	43.4	308.6	343 ± 1
9	10	100	128.3	45.7	310.9	351 ± 0.5
10	24	120	82.6	0	265.2	296 ± 1
Array Size: 2 x 2 x 3 (36,309 g Pu)						
11	49	76	387.4	304.8	957.3	255 ± 5
12	41	90	174.0	91.4	530.5	616 ± 2
13	36	120	118.1	35.6	418.8	460 ± 2
Array Size: 2 x 2 x 4 (48,422 g Pu)						
14	51	100	153.7	71.1	643.6	684 ± 2
15	63	141	95.3	12.7	468.3	421 ± 3
Array Size: 2 x 2 x 5 (60,541 g Pu)						
16	71	170	82.6	0	512.8	470.5 ±1
Array Size: 3 x 3 x 3 (81,754 g Pu)						
17	9 [c]	120.0	127.5	N/A	N/A	483 ± 2
18	10 [c]	127.0	127.5	N/A	N/A	584 ± 1
19	12 [d]	129.0	127.5	N/A	N/A	606.0 ± 0.5
20	13 [d]	129.0	127.5	N/A	N/A	606.8 ± 0.5
21	15 [e]	130.0	127.5	N/A	N/A	623.0 ± 0.5
22	16 [e]	130.0	127.5	N/A	N/A	629.1 ± 0.1
23	17 [e]	130.0	127.5	N/A	N/A	628.2 ± 0.3
24	18 [e]	130.0	127.5	N/A	N/A	630.8 ± 0.5
25	19	130.5	127.5	N/A	N/A	658.0 ± 0.5
26	22	128.0	131.0	N/A	N/A	656.0 ± 0.5

(a) Center-to-center spacing.
(b) Water heights are relative to the bottom of the tank for Cases 1-16 and to the bottom of the sleeve for Cases 17-26.
(c) These experiments remained subcritical when all available water was used. Their critical water heights were extrapolated from very high multiplication.
(d) The difference between these two experiments was that Experiment 12 (Case 19) had a long, thin neutron detector immersed in the water.
(e) The differences in these experiments were the way the sleeves were handled. Experiments 15 and 16 (Cases 21 and 22) had the sleeves rotated. Experiments 17 and 18 (Cases 23 and 24) used a systematic loading technique to keep all plutonium systematically to one side of the outer can.

II. Sensitivity Analysis

The method of the sensitivity analyses was similar for both sets of experiments. Each set of experiments was divided into several groups. One experiment in each group was chosen as a representative of that group and analysis was performed on the chosen experiment. The results were assumed to be applicable to the other experiments in that group due to the similarities. For most sensitivity studies of the

first set of experiments, groups were chosen based on the average energy of neutrons causing fission as determined using KENO-V.a with 27-group ENDF/B-IV cross sections. For other parameters, the groups were based on vertical or horizontal spacing. However, unless otherwise noted, grouping was based on average energy. For the second set, grouping was based on vertical and horizontal spacing.

For the first set, the experiments were divided into four groups: energy below 20 keV (Cases 8, 13, 14, and 15*), energy between 20 and 100 keV (Cases 6, 7, 9, 10*, 12, and 16), energy between 100 and 250 keV (Cases 2, 3*, 4, 5, and 11), and energy above 250 keV (Case 1*). The starred experiments were chosen as representative of that group. Analysis on other experiments in some groups was performed to confirm the appropriateness of the grouping. The second set of experiments was divided into six groups: Case 17, Case 18, Cases 19-20, Cases 21-24, Case 25, and Case 26. Analysis was done on Cases 17, 18, 19, 21, 25, and 26.

For each representative measurement, a base case was chosen. For the first set of experiments, this included the plutonium parts, the three aluminum plates of the trays, the water reflector, and the aluminum tank. For the cases in the second set, the plutonium parts, perforated aluminum sleeves and water reflector were modeled as the base case. For each base case a k_{eff} value was found. One parameter in the base case was then perturbed and the k_{eff} value was again calculated. The effect on k_{eff} due to a parameter was found by comparing the base case and the perturbed k_{eff} values. Most sensitivity studies were performed using MCNP with continuous energy ENDF/B-V cross section data. In some cases, KENO-V.a with 27-group ENDF/B-IV cross section was used. Parameters considered as part of this analysis include plutonium height and radius, plutonium mass/density, critical water height, lattice horizontal and vertical spacing, plutonium position within outer steel can, and water impurities.

II.A. Plutonium Height, Diameter, and Mass/Density

The plutonium metal cylinders used in both sets of experiments were taken from a larger set of 130 cylinders. The uncertainties on the average plutonium height and diameter of the larger set were reported to be ±0.15 mm and ±0.05 mm, respectively. To determine the uncertainty in k_{eff} due to these uncertainties, each parameter was adjusted independently by adding and subtracting the value of the uncertainty (a value of 0.025 mm was used for the radius). The resulting differences in k_{eff} were averaged for each parameter. The results of all sensitivity studies are given in Table 2.

For the 130 cylinders, the average plutonium density was reported with an uncertainty of ±0.08 mg/mm^3, which corresponds to an uncertainty of ±0.41%. For the second set of experiments, this value was used for plutonium density. The uncertainty in k_{eff} was found by perturbing the density by +0.5% and –0.5%. The average of the resulting differences was linearly scaled to correspond to an uncertainty of 0.41%.

For the first set of experiments, the individual masses of the plutonium metal used in the experiments were used to compute an uncertainty. The largest mass uncertainty for these arrays was found to be 0.28%. This value is used as the mass uncertainty in this analysis. Furthermore, since an analysis on volume is performed separately by analyzing height and diameter uncertainties, no sensitivity study on plutonium density due to the reported uncertainty is needed. However, an uncertainty of 0.1% was used for the plutonium density due to the plutonium being brought into equilibrium with the water reflector. During the experiment, the plutonium temperature was decreased from ~43°C to approximately 22°C.

II.B. Critical Water Height

Critical water heights for the acceptable experiments were reported with uncertainties between 0.5 and 5 mm for the first set and between 0.1 and 2 mm for the second set. For the first set, the uncertainty in k_{eff} for each group was determined by using the average uncertainty or the maximum uncertainty of that group (with a minimum uncertainty of 2 mm so that the difference in k_{eff} could be seen using MCNP). The critical water height was adjusted by increasing and decreasing the height by the amount of the uncertainty. The resulting differences in k_{eff} were averaged. The uncertainty in k_{eff} for each case was found by linearly scaling the result of the representative case to correspond to the individual uncertainty. The method for the second set was the same as above. The uncertainty reported for the representative case was used as the uncertainty value with a minimum of 2 mm. The results of the 2 mm analysis were linearly scaled to correspond to the correct uncertainty when necessary.

An additional uncertainty in critical water height existed for each set of experiments due to the uncertainty in the amount of water below the lowest plutonium can. Although it is expected that the small differences have a negligible effect for bottom reflector thickness, it does contribute to the critical water height uncertainty since all heights are given relative to the bottom of the experimental tank. For the first set, the feet of the support structure were reported in reference 1 to be 102 mm long. However, the feet were manufactured in English units and were 4 inches long (101.6 mm). Furthermore, the top tray heights given in reference 1 were calculated using a bottom reflector thickness (i.e. foot length) of 100 mm. Since it is not certain which value is more accurate, a value of 100.8 (the average of the English and the value used in calculations) is used in the benchmark model with an additional uncertainty in critical water height of ±0.8 mm. For the second set, the bottom plutonium can was reported to be 251 mm above the bottom of the sleeve. Using a frame thickness of 12.7 mm, the bottom can was located 263.7 mm above the tank bottom. However, measurements indicate that this value was actually 261 mm. Therefore, due to this inconsistency, an additional uncertainty of ±2.7 mm is needed for the critical water height.

II.C. Lattice Spacing

For both sets of experiments the horizontal and vertical lattice spacing contributed to the uncertainty in k_{eff}. Although, no spacing was reported with an uncertainty, uncertainties in these parameters arose from discrepancies in the reported data. For the horizontal spacing of the first program, the uncertainty was caused, in part, by the conversion from English to metric units. The horizontal spacing was determined by the pre-cut holes in the middle aluminum plate of the trays and was reported to a tenth of a centimeter. However, the original dimensions etched on the trays were in English units. When converted to millimeters the dimensions of the trays were as follows: 89.916 mm for the 90 mm spacing, 100.584 mm for the 100 mm spacing and 119.888 mm for the 120 mm spacing. Since it is not known which dimension was more accurate, the horizontal spacing is taken to be an average of the reported value and the converted English value, as recommended by the experimenter.[3] This method leads to a systematic uncertainty of ±0.04 mm for the 90 mm spacing, ±0.29 mm for the 100 mm spacing and ±0.06 mm for the 120 mm spacing. No average value or systematic uncertainty was needed for the 76 mm spacing since these cans were close-packed. The average values were determined using values reported to an accuracy of 1 mm and .01 inch which corresponds to ±0.5 mm and ±0.127 mm for the random horizontal spacing uncertainty, respectively. The random uncertainty due to averaging is, therefore, ±0.26 mm. An additional random horizontal uncertainty exists due to the "slip fit" of the plutonium cans into the holes of the middle plates of the trays. The holes were reported to be 76.3 mm while the plutonium cans were only 76.2 mm. Therefore an uncertainty of ±0.05 mm is combined with the ±0.26 mm uncertainty to give a total random horizontal spacing uncertainty of ±0.26 mm. The energy grouping described earlier was not used for this parameter. Instead, a sensitivity study was performed on an experiment for each different horizontal spacing. (Cases 1 and 3, ΔX=76 mm; Case 6, ΔX=90 mm; Case 9, ΔX=100 mm; Case 10, ΔX=120 mm; Case 15, ΔX=141 mm; and Case 16, ΔX=170 mm). For the remainder of the experiments, the result corresponding to the horizontal spacing was used regardless of energy group. For all cases with a horizontal spacing of 76 mm, the result from Case 3 was used except for Case 1. A separate analysis was performed on Case 1.

The vertical spacing uncertainty for the first set of experiments was determined by placing spacer shims between trays. The shims were manufactured with lengths of 2.54 mm and in 5.08 mm increments up to 50.8 mm. The shims were measured and carefully maintained to be free of dirt and burrs. It was, therefore, believed that the reported vertical spacings could be "accepted with good confidence." The average reported uncertainty for the lengths of spacer shims was reported to be ±0.02 mm. Approximately four spacer shims per corner were used between trays. Using these values, the random uncertainty in vertical spacing from the uncertainty in spacer lengths is $\sqrt{4}x0.02x\sqrt{(N-1)}$, where N is the number of trays. This uncertainty is not needed for the experiments in which no shims were used (i.e. experiments in which a tray was placed directly on the lower tray).

An additional uncertainty in the vertical spacing for Set 1 arises from the discrepancy in tray height. The reported value of the tray height is 82.55 cm. However, using a value of 6.35 cm for each plate and 69.47 mm for the height of the plutonium and assuming that the top plate lay directly on the plutonium can, the tray height would be 82.17 mm. The difference between these two values gives an additional vertical spacing uncertainty of $\pm 0.35x\sqrt{N}$ mm due to tray height. For all vertical spacing sensitivity studies, the water height was maintained constant with respect to the bottom of the tank. The uncertainty due to spacer

length and the uncertainty due to tray height were combined quadratically to find the uncertainty in vertical spacing. As with the horizontal uncertainty sensitivity study, the four groupings described in Section II.A are not used for this parameter. Instead, the cases were grouped according to vertical spacing (Cases 10 and 16, ΔZ=82.55 mm; Case 15, ΔZ=95.3 mm; Cases 7 and 5, 100 mm<ΔZ<110 mm; Cases 13, 8, and 9, 110<ΔZ<130 mm; Cases 1 and 6, 130<ΔZ<150 mm; Cases 14, 12, and 2, 150<ΔZ<200 mm; Cases 3 and 4, 200<ΔZ<250 mm; and Case 11, ΔZ>250 mm). The sensitivity study was performed on the case which had the smallest vertical spacing in that group. (Cases 10, 16, 15, 7, 13, 1, 14, 3 and 11). For the cases in which the tray was placed directly on the lower tray (Cases 10 and 16), the vertical spacing uncertainty was determined by adjusting the tray thickness and taking the difference between the two cases.

For the second set, lattice spacing uncertainty results from the spacing of the holes in the perforated aluminum sleeves. The horizontal spacing was controlled accurately by the experimenters and no uncertainty in k_{eff} was found due to the reported horizontal spacing. The vertical spacing was determined by placing steel pins in the holes of the perforated aluminum sleeves. The experimenters were careful to locate the sleeve holes to assure the same vertical location in each column. This method assures reproducibility of the vertical spacing. The holes in the sleeves were reported as 3.2-mm-diameter holes on 4.8-mm center in a triangular pattern. The experimenter reported[2] that the holes were actually 1/8-inch-diameter holes in a 3/16-inch triangular pitch. This discrepancy leads to a difference of 0.36 mm in the 12.75-cm vertical separation and 0.98 mm in the 13.10-cm vertical separation. These differences were assumed for the uncertainty in vertical spacing. The spacing was increased and decreased by these amounts, and the computed difference in k_{eff} was divided by two to find the uncertainty in a single movement.

II.D. Plutonium Position

For each set of experiments, the same plutonium metal cylinders were used. The plutonium metal was contained within two cans. The inner aluminum can fit snugly around the plutonium and allowed little, if any, movement of the plutonium. The aluminum can was then sealed within an outer stainless steel can. The dimensions of the outer can were large enough to allow the inner can to move. It is not known where the inner can was within the outer can during an experiment although it is believed that the inner can would seek about the center. However, there is still some uncertainty. In the base-case models, the plutonium metal is centered within the cans.

For the first set of experiments, the effect of the uncertainty in the location of the plutonium metal was found by moving all of the aluminum cans toward the center of the array and away from the center of the outer can by the width of the air gap. To account for a random uncertainty in the plutonium position of a can, the average of the differences in k_{eff} was then divided by the square root of the number of plutonium parts. Since the sensitivity to the plutonium can spacing is dependent on the horizontal spacing (i.e. the smaller the ΔX, the larger the effect), the same grouping used for the horizontal spacing uncertainty for Set 1 was also used for this parameter.

For the second set of experiments, an indication of the uncertainty in k_{eff} due to the position of the plutonium within the outer steel can was given by the results of Cases 21 and 22 of Set 2. Case 22 was a repeat of Case 21 with the sleeves rotated through a certain angle. The difference in critical water heights for these two measurements was 6.1 mm. The calculated difference in k_{eff} was 0.0012. This values is used for the effect of the uncertainty in horizontal spacing for Cases 17-20 and 21.

For experiments performed after Case 22, a systematic loading technique was used. It was designed to keep all plutonium to one side of the outer can, reducing any random error due to the shifting of the plutonium inside the outer steel can. This technique involved loading the same cylinders into the same sleeves and orienting all sleeves in the same direction as determined by their weld beads. Also, just before rotating the sleeves into a vertical position, the sleeve was tapped to move the plutonium cans to the same side. Therefore, for Cases 25 and 26, the changes in k_{eff} due to plutonium position within the outer steel can were found by moving all of the aluminum cans in the outer layer toward the center of the array by the width of the air gap. The three aluminum cans in the center sleeve remained centered in their outer cans. For Cases 25 and 26, the changes in k_{eff} were 0.0039 and 0.0041, respectively. These values clearly overestimate the effect of random movement of each piece. To account for a random uncertainty in the plutonium position of a can, the computed difference in k_{eff} was then divided by the square root of the number of plutonium parts.

II.E. Water Impurities and Other Effects

The water used for the experiments was regular tap water at room temperature. At the time of the experiments, the water was not analyzed for content. However, the laboratory water was sampled at various times and the result of one analysis is listed in Table 4 of Part I of this paper. Also, it is stated in reference 1 that the water properties "neither change much seasonally nor over a span of years; so the tabled data is considered representative." Other impurities arose from the treatment of the water at Rocky Flats; however, these were not well specified and were already present in the water in some form before arriving at Rocky Flats. Therefore, these impurities were not included in this analysis and are assumed to have an insignificant effect. To find the effect on k_{eff} due to water impurities, the impurities from the table were added to the water and found to be statistically insignificant.

Other effects, such as the uncertainty in americium-241 content in the plutonium and iron content in the stainless steel, were analyzed and found to be insignificant. For all structural materials, average and typical values for density and isotopic content were used. It is assumed that small variations in the composition would be negligible.

All parameters discussed in this section are considered as a single uncertainty and included at the level of the one standard deviation uncertainty of the calculations, $\Delta k_{eff} = 0.0008$.

II.F. Combination of Uncertainties

Table 2 shows the results of all sensitivity studies for Set 1 and Set 2. For each group of experiments, a combined uncertainty due to measurement uncertainties was computed by combining the individual uncertainties as the square root of the sum of the squares. In addition to the values listed, an uncertainty of $\Delta k_{eff} = 0.0008$ (the value of the Δk standard deviation associated with the MCNP calculations) was included for all cases for the water impurities and other effects.

III. Benchmark Model

III.A. Simplification Effects

The benchmark model for the first set of experiments consists of the double-canned plutonium metal parts, the aluminum plates of the trays, the water reflector, and the aluminum tank. The benchmark model for Set 2 includes the plutonium parts, the aluminum sleeves and the water reflector. The room and parts of the support structure were not included. Therefore, to find the effect of room-return neutrons, several components of the tank and room were modeled, in addition to the room walls, ceiling, and floor. For the first set of experiments, the corner rods, feet, spacers between plates, spacer shims between trays, and hold-down tubes were modeled as described in Section III.B.1 of Part I. The feet extended from the bottom of the lower tray to the top of the tank bottom. The hold-down tube extended from the top of the top tray to the top of the corner rods. The spacers between the bottom plate and the middle plate and between the middle plate and the top plate were also included.

Since the water around and beneath the plutonium parts was not effectively infinitely thick and since the top layer of plutonium was exposed for some experiments (two layers were exposed for Case 11), several structures in the room were also included in the model. The horizontal split table, the water reservoir, the three-sided shield, and the closest wall of the fissile solution containment room were modeled as described in Section III.D of Part I.

Also included in the room return analysis was the top stiffening ring of the experimental tank and an aluminum water heater that was present in the room at the time of the experiments. The water heater was modeled with a height that extended from the top of the water reservoir to 20 cm below the top of the experiment tank. The water reservoir was located 0.3 m beneath the tank with its long dimension

Table 2. Results of Sensitivity Study All Experiments. [(a)]

Case #	Parameter								
	Pu mass	Pu density	Pu height	Pu diameter	Pu spacing	Horizontal Spacing	Vertical Spacing	Water Height	Combination[d]
Set 1 – 2x2xN Arrays									
1	0.0017	0.0006	0.0012	(b)	0.0036	(c)	0.0003	0.0004	0.0043
2	0.0018	0.0006	0.0011	(b)	0.0035	(c)	0.0009	(b)	0.0043
3	0.0018	0.0006	0.0011	(b)	0.0035	(c)	(b)	(b)	0.0042
4	0.0018	0.0006	0.0011	(b)	0.0035	(c)	(b)	(b)	0.0042
5	0.0018	0.0006	0.0011	(b)	0.0025	0.0003	0.0010	(b)	0.0036
6	0.0019	0.0007	0.0016	0.0010	0.0025	0.0003	0.0003	0.0006	0.0039
7	0.0019	0.0007	0.0016	0.0010	0.0019	0.0007	0.0010	0.0008	0.0037
8	0.0018	0.0007	0.0012	(b)	0.0019	0.0007	0.0005	0.0003	0.0032
9	0.0019	0.0007	0.0016	0.0010	0.0019	0.0007	0.0005	0.0006	0.0036
10	0.0019	0.0007	0.0016	0.0010	0.0016	0.0002	(b)	0.0004	0.0033
11	0.0018	0.0006	0.0011	(b)	0.0029	(c)	(b)	(b)	0.0037
12	0.0019	0.0007	0.0016	0.0010	0.0020	0.0003	0.0010	0.0013	0.0039
13	0.0018	0.0007	0.0012	(b)	0.0013	0.0002	0.0006	0.0004	0.0029
14	0.0018	0.0007	0.0012	(b)	0.0013	0.0007	0.0012	0.0004	0.0031
15	0.0018	0.0007	0.0012	(b)	0.0010	0.0005	0.0017	0.0006	0.0032
16	0.0019	0.0007	0.0016	0.0010	(b)	(b)	0.0023	0.0008	0.0038
Set 2 – 3x3x3 Arrays									
17	N/A	0.0027	0.0014	0.0016	0.0012	(b)	0.0010	0.0014	0.0041
18	N/A	0.0024	0.0010	(b)	0.0012	(b)	0.0020	0.0012	0.0038
19-20	N/A	0.0016	0.0010	(b)	0.0012	(b)	0.0016	0.0016	0.0033
21-24	N/A	0.0019	0.0015	(b)	0.0012	(b)	0.0009	(b)	0.0030
25	N/A	0.0025	0.0017	(b)	0.0008	(b)	0.0009	(b)	0.0034
26	N/A	0.0020	0.0014	(b)	0.0008	(b)	0.0017	(b)	0.0032

(a) The maximum one standard deviation uncertainty in the Δk results from the Monte Carlo calculations is 0.0008. Any numbers reported in the table which are below this value had standard deviations less than the difference due to linearly scaling the difference and its standard deviation to correspond to the correct uncertainty.
(b) These uncertainties were within the MCNP statistical limitation of the difference in k_{eff} and are included with the 0.0008 uncertainty described in the preceding paragraph.
(c) No uncertainty was needed for the systematic uncertainty and its related random uncertainty for close-packed arrays (Δx=Δy=76 mm).
(d) The combination value includes the 0.0008 uncertainty as described in the paragraph preceding the table and uses the scaled values for the critical water height uncertainty.

perpendicular to the east wall. The slope of the bottom of the reservoir was ignored. To conserve volume, the reservoir was modeled with a depth of 0.3685 m. The amount of water left in the reservoir was found by subtracting the amount of water in the tank from the capacity of the reservoir (430 liters).

For the second set of experiments, the structures inside the plastic tank were modeled as described in Section III.B.2 of Part I, including aluminum framework, plastic disks, top and bottom aluminum bars, and top aluminum blocks. The framework was divided into three sections: the solid bottom with slots, the four open-faced sides and the open-faced slotted top. All structures were modeled as pure aluminum. When necessary, the aluminum density was reduced to account for neglecting slots in the structures.

The framework was centered inside the plastic tank with inner dimensions of 71.1 x 71.1 cm. The tank walls were modeled with a thickness of 9.95 cm and a height of 101.6 cm. The walls were made of methyl methacrylate . A typical composition of methyl methacrylate is as follows: 8.03 weight percent hydrogen, 59.72 weight percent carbon, 32.14 weight percent oxygen, and 0.11 weight percent other. This composition was used in this analysis with a density of 1.18 g/cm^3. The bottom of the tank was modeled as a pure aluminum square slab with a thickness of 1.91 cm and length of 91 cm.

For this set, the water around and beneath the plutonium parts was effectively infinitely thick (minimum thickness of 12.7 cm). Therefore, it was assumed that all structures in the room would

contribute negligibly to room return neutrons. The location of the tank in the room was modeled as described in Section III.D of Part I.

For both sets of experiments, the walls, floor, and ceiling were also modeled as part of the room return analysis. These were modeled using ordinary concrete composition with the atom densities in Table 3. The rebar in the concrete is accounted for by increasing the iron atom density by an amount which added an additional 7000 kg of iron to the walls, floor, and ceiling. This amounted to an increase of 3% in the concrete density. The room walls and ceiling were modeled with dimensions found in Section III.D of Part I. For the floor, the thickness of the concrete was increased to 1 m to account for some of the earth beneath the floor.

This analysis showed that, for all but one case, the room return effect was statistically insignificant. The difference in k_{eff} between the benchmark model and the room return case was less than the calculation uncertainty (<0.0008) for all cases except Case 17. For Case 17, this difference was 0.0026 ± 0.0008.

Table 3. Composition of Concrete Used in Analysis. [(a)]

Element	Concrete (atom/barn-cm)	Concrete with Rebar (atom/barn-cm)
H	8.3094 E-3	8.3094 E-3
O	5.9233 E-2	5.9233 E-2
Ca	2.6714 E-3	2.6714 E-3
Si	2.3732 E-2	2.3732 E-2
Fe	4.5618 E-4	1.4493 E-3
Al	2.4359 E-3	2.4359 E-3
Na	1.2280 E-3	1.2280 E-3

(a) Composition is standard material from the MCNP manual with the density increased to 3.07 g/cm^3, due to the additional Fe. Since the walls have little effect on k_{eff}, it is assumed that variations in the concrete composition are negligible.

III.B. Geometry and Material

As mentionned previously, the benchmark model for the first set of experiments consists of the double-canned plutonium metal parts, the aluminum plates of the trays, the water reflector, and the aluminum tank. For Set 2, the benchmark model includes the plutonium parts, the aluminum sleeves and the water reflector.

The plutonium metal height and radius are 4.633 cm and 3.2625 cm, respectively. The plutonium density was calculated for all experiments using total mass and volume of the plutonium parts used in the individual experiments. Impurities were not included in the plutonium metal. Calculations show that neglecting the impurities has a statistically insignificant effect on the value of k_{eff}. Therefore, after subtracting the impurities, the plutonium density of the plutonium was calculated to be 19.54 g/cm^3 for the 2x2x2 arrays, 19.52 g/cm^3 for the 2x2x3 arrays, 19.53 g/cm^3 for the 2x2x4 and 2x2x5 arrays, and 19.54 g/cm^3 for the 3x3x3 arrays (Set 2). Also since the isotopic concentration of the plutonium was measured in 1965, the ^{241}Pu content was adjusted to account for the buildup of ^{241}Am from the time of measurement to a time during which these experiments were performed (from July 1965 to January 1975 for Set 1 and from July 1965 to May 1982 for Set2). The ^{241}Am is included in the benchmark model. Atom densities for the plutonium and americium isotopes are listed in Table 4.

The inner can is made of 1100 aluminum. It fits tightly around the plutonium metal and has a thickness of 0.037 cm, resulting in an outer radius of 3.2995 cm. This value is slightly smaller than the value found in reference 1 since a small air gap exists between the plutonium metal and the aluminum can. The effect of neglecting this gap is assumed to be negligible. The bottom of the inner aluminum can is 0.087 cm thick. The top of this can is 0.021 cm thick and is made of mild steel. The atom densities of all aluminum and steel materials used in the benchmark models are found in Table 5.

Table 4. Atom Densities for Plutonium Metal (atoms/barn·cm).

Isotope	Cases 1 - 10 (2x2x2)	Cases 11 - 13 (2x2x3)	Cases 14 - 16 (2x2x4, 2x2x5)	Cases 17-26 (3x3x3)
^{239}Pu	4.6054E-02	4.6007E-02	4.6031E-02	4.6054 E-02
^{240}Pu	2.9264E-03	2.9234E-03	2.9249E-03	2.9264 E-03
^{241}Pu	1.4214E-04	1.4199E-04	1.4207E-04	9.9882 E-05
^{242}Pu	4.8613E-06	4.8563E-06	4.8588E-06	4.8613 E-06
^{241}Am	8.2409E-05	8.2325E-05	8.2367E-05	1.2467 E-04

Table 5. Atom Densities of Structural Materials (atoms/barn-cm).

	Inner Can	Inner Can Lid	Outer Can	Trays, Tank	Sleeves
Material	3004 Al	Mild Steel[a]	304L Stainless Steel [b]	6061 Al [c]	3003 Al [d]
Al	5.8311 E-02			5.8183 E-02	3.5358 E-02
C		3.1547 E-04	1.1883 E-04		
Cr			1.7384 E-02	6.2542 E-05	
Cu	6.4442 E-05			6.3968 E-05	3.0891 E-05
Fe	2.0531 E-04	8.4131 E-02	5.7902 E-02	2.0380 E-04	1.2302 E-04
H [e]					2.6894 E-02
Mg	7.0764 E-04			6.6898 E-04	
Mn	3.7270 E-04	3.1899 E-04	1.7319 E-03	4.4395 E-05	2.1438 E-04
Ni			8.1061 E-03		
O [e]					1.3447 E-02
P		2.2937 E-05			
S		3.6922 E-05			
Si	1.7497 E-04	1.6864 E-05	1.6939 E-03	3.4736 E-04	2.0968 E-04
Sn		1.1970 E-04			
Ti				5.0939 E-05	
Zn	6.2625 E-05			6.2164 E-05	1.5048 E-05
Density (g/cm^3)	2.72	7.865	7.9	2.70	1.63

(a) The composition of mild steel is from References 1 and 2 and listed in Table 5. The density is an average of several mild low-carbon steels from the handbooks.
(b) The weight percents used for 304L stainless steel were 0.03% for C, 19% for Cr, 67.97% for Fe, 2% for Mn, 10% for Ni, and 1% for Si.
(c) The weight percents used for 6061 aluminum were 96.55% for Al, 0.2% for Cr, 0.25% for Cu, 0.7% for Fe, 1% for Mg, 0.15% for Mn, 0.6% for Si, 0.15% for Ti, and 0.25% for Zn.
(d) The weight percents used for 3003 aluminum were 97.2% for Al, 0.2% for Cu, 0.7% for Fe, 1.2% for Mn, 0.6% for Si, and 0.1% for Zn.
(e) Hydrogen and oxygen for the submerged parts of the aluminum sleeve for Set 2 experiments.

The outer can has an outer radius of 3.81 cm and an outer height of 6.947 cm. The can is made from Type 304L Stainless Steel. The thickness of the can is 0.34 cm on the sides, 0.67 cm on the top, and 0.91 cm on the bottom. The aluminum can rests on the bottom of the outer steel can and is centered in the outer steel can, resulting in an gap between the two cans of 0.1705 cm on the sides and 0.626 cm on top.

The aluminum plates for the first set of experiments are 45.7 cm square. The bottom of the middle plate is 3.06 cm from the top of the bottom plate while the bottom of the top plate is 3.29 cm from the top of the middle plate. All plates are 0.635 cm thick and made of Type 6061 aluminum. The rounded corners of the plates were neglected. The effect of doing this is assumed to be negligible. The holes in the middle plate fit snugly around the plutonium with a diameter of 7.62 cm. The hole diameter was reported as 7.63

cm in Reference 1. Using this, a small gap around the plutonium cans of 0.005 cm would exist. This is also considered negligible and is not included in the benchmark model. The plutonium cylinders are placed in the holes of the middle plates in the patterns shown in Figure 2 of Part I. Holes in the middle plate that are not occupied by plutonium cylinders are filled with water or void, depending on the critical water height. For the cases in which the plutonium cans are touching, a large square, 15.24 cm sides, was cut into the middle plate, instead of holes. This was just large enough to fit four plutonium parts. The space around the plutonium is filled with water or void, depending on the critical water height.

The tank for this set of experiments was made from Type 6061 aluminum. The tank has an inner radius of 34.925 cm and a thickness of 0.635 cm. The bottom is also Type 6061 aluminum with a thickness of 0.635 cm. The tank inside height is 125 cm. The bottom of the lowest tray is 10.08 cm above the tank bottom, as described in Section II.B.

For the second set of experiments, the support structure consisted of perforated aluminum sleeves. The sleeves were modeled as pure aluminum with reduced density of 1.63 g/cm^3. For the parts of the sleeves that were submerged in water, the aluminum and water were homogenized. The sleeves fit tightly around the outer steel can with a thickness of 0.16 cm (outer diameter of 7.94 cm). The sleeves are 91.4 cm in height. The lowest can was 25.1 cm from the bottom of the sleeve. The water reflector is square and extends 35.55 cm in each horizontal direction, measured from the center of the middle can. Water floods the array from the bottom of the sleeve to the critical water height. The tank is not part of the benchmark model for this set of experiments.

The water used in both sets of experiments was regular tap water with a density of 0.9982 g/cm^3. No water impurities are included in the benchmark model. The atom densities for the water reflector are given in Table 6.

Table 6. Atom Densities for Water Reflector.

Element	atom/barn-cm
H	6.6735 E-02
O	3.3368 E-02

The center-to-center spacings and the critical water heights for all benchmark experiments are listed in Table 7. The pattern in which the plutonium cans were loaded into a tray can be found in Figure 2 of Part I of this paper. The third column of Table 7 gives the spacing between the holes in the tray as used in the benchmark model. These values are not the same as the values found in Figure 2 of Part I for the reasons discussed in Section II.C of this paper.

Since Cases 19 and 20 of Table 1 are effectively the same experiment, Case 19 is used as the benchmark model. The difference between these two cases was that Case 19 had a long, thin neuton detector immersed in the water. However, the detector had a negligible effect and the critical water heights of these experiments are not significantly different. Therefore, Case 19 is acceptable as a benchmark model. The detector is not part of the benchmark model.

Cases 21-24 of Table 1 all used the same horizontal and vertical spacing. The differences among these experiments were the way in which the plutonium pieces were loaded and the sleeves oriented during an experiment. The critical water heights for these measurements ranged between 62.3 cm and 63.08 cm. The benchmark model uses an average critical water height of 62.78 cm. The uncertainty associated with using the range in water heights was combined in the sensitivity study as the uncertainty due to plutonium spacing. The sensitivity studies on Case 21 are assumed to be applicable to the benchmark model since all parameters are the same except for the critical water height. This benchmark experiment appears in Table 7 as Benchmark Case 20. Cases 25 and 26 of Table 1 are also renumbered in Table 7 as Benchmark Cases 21 and 22, respectively.

Table 7. Horizontal and Vertical Center-to-Center Spacings and Critical Water Heights.

Benchmark Case #	Horizontal Cylinder Spacing (mm)[a]	Horizontal Spacing of Holes[b] ΔX = ΔY (cm)	Vertical Spacing [c] ΔZ (cm)	Water Height (cm)
2x2x2 arrays				
1	76	[d]	13.335	20.2
2	76	[d]	18.415	23.5
3	76	[d]	21.465	24.6
4	76	[d]	23.495	46.3
5	90	8.996	10.795	23.55
6	90	8.996	13.335	30.88
7	100	10.029	10.058	26.3
8	100	10.029	12.595	34.3
9	100	10.029	12.825	35.1
10	120	11.994	8.255	29.6
2x2x3 arrays				
11	76	[d]	38.735	25.5
12	90	8.996	17.395	61.6
13	120	11.994	11.815	46.0
2x2x4 arrays				
14	100	10.029	15.365	68.4
15	141	10.029	9.525	42.1
2x2x5 arrays				
16	170	11.994	8.255	47.05
3x3x3 arrays				
17	12.00	N/A	12.75	48.30
18	12.70	N/A	12.75	58.40
19	12.90	N/A	12.75	60.60
20 [e]	13.00	N/A	12.75	62.78
21 [e]	13.05	N/A	12.75	65.80
22 [e]	12.80	N/A	13.10	65.60

(a) Nominal spacing only.
(b) Holes in middle plate. See Figure 2 of Part I for Pu cylinder placement. The values in this column were suggested by the experimenter as an average of two numbers.[3]
(c) The vertical spacing is the distance from the bottom of one tray to the bottom of the above tray, not the distance between trays. It is the sum of the reported spacing between trays in Table 1 and the 8.255-cm tray height.
(d) Four canned Pu cylinders close-packed in one hole 15.24 cm square.
(e) These benchmark cases were renumbered. Benchmark Case 20 uses the average critical water height of Cases 21-24 of Table 1 (see discussion in text). Benchmark Cases 21 and 22 were Cases 25 and 26 of Table 1.

III.C. Benchmark K_{eff}

All experiments discussed in this paper were approach-to-critical with small extrapolations to critical or critical experiments. Therefore, the experimental k_{eff} value for all experiments is 1.0000.

The room return analysis discussed in Section III.A showed that the only correction needed to the benchmark k_{eff} value was for Case 17. For the rest of the experiments, the computed room return corrections were statistically insignificant. The correction for room return for Experiment 1 is 0.0026, resulting in a benchmark model k_{eff} value of 0.9974 for this experiment. For all experiments, the calculation uncertainty value, 0.0008, was combined with the uncertainty found in Section II.F. The final uncertainty values for each experiment are listed in Table 8 along with the benchmark model k_{eff} values.

Table 8. Benchmark k_{eff}.

Benchmark Case #	Benchmark k_{eff}	Uncertainty
2x2x2 arrays		
1	1.0000	0.0044
2	1.0000	0.0044
3	1.0000	0.0043
4	1.0000	0.0043
5	1.0000	0.0037
6	1.0000	0.0040
7	1.0000	0.0038
8	1.0000	0.0033
9	1.0000	0.0037
10	1.0000	0.0034
2x2x3 arrays		
11	1.0000	0.0038
12	1.0000	0.0040
13	1.0000	0.0030
2x2x4 arrays		
14	1.0000	0.0032
15	1.0000	0.0033
2x2x5 arrays		
16	1.0000	0.0039
3x3x3 arrays		
17	0.9974	0.0042
18	1.0000	0.0038
19	1.0000	0.0033
20	1.0000	0.0030
21	1.0000	0.0034
22	1.0000	0.0032

IV. Discussion

IV.A. Spectrum

It was desired, for naming purposes, to classify these systems as thermal, intermediate, or fast, depending on the average energy of neutrons causing fission. To do this, KENO-V.a with 27-group ENDF/B-IV cross section data was used. For both sets of experiments, it was found that the majority of fissions was caused by fast neutrons (those having energy greater than 100 keV). Therefore, even though the arrays are at least partially water-reflected, they are fast spectrum assemblies. This result is explained by the fairly large plutonium parts, approximately 3 kg each, used in the experiments.

IV.B. Code and Cross Section Evaluation

A k_{eff} value for each benchmark experiment described in Section III was found using MCNP with continuous energy ENDF/B-V and ENDF/B-VI cross sections and KENO-V.a with 27-group ENDF/B-IV cross section data. The results are listed in Table 9. For all codes and cross section sets, the k_{eff} value for Case 17 is overestimated by more than 1%. This is the only case for which this occurs. The reason for the discrepancy is unknown, however there were two differences between this experiment and the rest of the

experiments in Phase II: the top layer of plutonium was above the critical water height and the extrapolation to critical was greatest for Case 17.

Table 9. K_{eff} Values for Benchmark Experiments.

Benchmark Case #	MCNP (continuous energy ENDF/B-V)[a]	MCNP (continuous energy ENDF/B-VI)	KENO-V.a (27-group ENDF/B-IV)
2x2x2 arrays – Phase I			
1	1.0037 ± 0.0008	1.0028 ± 0.0008	0.9999 ± 0.0017
2	1.0008 ± 0.0008	1.0000 ± 0.0008	0.9947 ± 0.0017
3	0.9996 ± 0.0007	0.9971 ± 0.0007	0.9943 ± 0.0017
4	1.0030 ± 0.0008	1.0010 ± 0.0008	1.0044 ± 0.0017
5	1.0030 ± 0.0008	0.9988 ± 0.0007	1.0014 ± 0.0018
6	1.0000 ± 0.0008	0.9981 ± 0.0007	1.0005 ± 0.0017
7	1.0028 ± 0.0007	0.9993 ± 0.0008	1.0010 ± 0.0016
8	1.0015 ± 0.0008	1.0009 ± 0.0008	1.0008 ± 0.0016
9	1.0001 ± 0.0008	0.9979 ± 0.0008	0.9990 ± 0.0018
10	1.0028 ± 0.0007	1.0007 ± 0.0008	1.0026 ± 0.0017
2x2x3 arrays – Phase I			
11	0.9963 ± 0.0008	0.9960 ± 0.0008	0.9919 ± 0.0019
12	0.9985 ± 0.0008	0.9981 ± 0.0008	0.9988 ± 0.0018
13	0.9985 ± 0.0008	0.9980 ± 0.0008	0.9954 ± 0.0016
2x2x4 arrays – Phase I			
14	1.0035 ± 0.0008	1.0034 ± 0.0008	1.0042 ± 0.0017
15	1.0038 ± 0.0008	0.9999 ± 0.0008	1.0043 ± 0.0016
2x2x5 arrays – Phase I			
16	1.0052 ± 0.0008	1.0030 ± 0.0008	1.0048 ± 0.0016
3x3x3 arrays – Phase II			
17	1.0152 ± 0.0008	1.0134 ± 0.0007	1.0105 ± 0.0016
18	1.0024 ± 0.0008	1.0011 ± 0.0008	1.0048 ± 0.0017
19	1.0005 ± 0.0008	0.9998 ± 0.0008	1.0031 ± 0.0016
20	1.0014 ± 0.0008	0.9994 ± 0.0008	0.9986 ± 0.0016
21	0.9979 ± 0.0008	0.9979 ± 0.0008	0.9987 ± 0.0015
22	1.0022 ± 0.0008	1.0011 ± 0.0008	1.0010 ± 0.0015

[a] All cross sections used for ENDF/B-V data were xxxxx.50c cross sections, except for ^{239}Pu. For this isotope, the recommended cross section, 94239.55c, was used.

Bias values were calculated for each code/cross section set. It is recognized that these bias values are for a very limited set of data and are not intended as a validation of the codes used. Therefore, any conclusions drawn in this section are for these particular systems only. More data would be needed for a true validation.

For this analysis, bias values are defined as $\Delta k_{avg} \pm$ spread (uncertainty), where Δk_{avg} is the average difference between the calculated and benchmark k_{eff} values, $\Delta k_{avg} = (1/n)\Sigma_{i=1}^{n}(k_{cal.i} - k_{bench,i})$, where n is the number of experiments, the spread is the spread about the average calculated k_{eff} value (which is the same as the standard deviation in Δk_I), $spread = sqrt\{(\Sigma_{i=1}^{n}(k_{calc,i} - k_{calc,avg})^2)/(n-1)\}$, and the uncertainty is the statistical uncertainty due to the calculation and the benchmark uncertainty, $uncertainty = \{(1/n)sqrt(\Sigma_{i=1}^{n}(s_{calc,i}^{2} + s_{bench,i}^{2}))\}$.

Bias values for the experiments grouped according to plutonium mass, horizontal spacing, vertical spacing, hydrogen to plutonium ratio, or average energy of neutrons causing fission are given in Tables 10-14 and the average Δks are plotted in Figures 1-5, respectively. In some cases, Case 17 is excluded from the bias calculation since it is not known why the k_{eff} value for this experiment is significantly overestimated relative to the rest of the experiments. In all cases, excluding this experiment greatly decreases the bias for all codes. In addition, the Δk_{avg} values calculated without this case are plotted in the figures.

Using Figure 1, no significant trend can be seen in the bias values with increasing plutonium mass. The 2x2x4 and 2x2x5 arrays have larger absolute values of Δk_{avg} than do the other arrays (not considering Case 17). This would seem to imply that for these arrays, the bias is larger. However, only three experiments are included in both of these sets (2 experiments in the 2x2x4 array set and 1 experiment in the 2x2x5 array set). Therefore the uncertainty in the bias values is large and the bias values are statistically within the range of the other arrays. In general, MCNP with ENDF/B-VI cross sections has smaller bias values than the other two codes/cross sections sets.

The Δk_{avg} values versus horizontal spacing are plotted in Figure 2. Case 17 is not included in this figure. Also, for simplification and clarity, five experiments with horizontal spacing between 127 and 130.5 mm are averaged together. A bias is calculated for this average spacing (128.9 mm) using the five experiments. For MCNP with ENDF/B-V and KENO with ENDF/B-IV, the Δk_{avg} appears to increase for the largest two spacings. However, for both of these spacings, there is only one experiment contributing to the bias. For MCNP with ENDF/B-VI, the Δk_{avg} is highest for the largest spacing but is still within the uncertainty value. Thus no trend is seen for this code/cross section. In general, all Δk_{avg} values are within the uncertainty of the bias values. The bias calculated using MCNP with ENDF/B-VI cross sections have lower absolute values of Δk_{avg} and a smaller spread than do the bias using the other two codes/cross section libraries.

The experiments were grouped on a per centimeter basis for calculation of a bias versus vertical spacing. The bias values are shown in Table 12 and plotted in Figure 3. The vertical spacings shown are the average for that group. Case 17 is not included in the analysis. Again, no trends can be seen in Figure 3 and the Δk_{avg} values are, for the most part, within the uncertainty of the bias. As with the plutonium mass and horizontal spacing groupings, the Δk_{avg} values are smallest, in general, for MCNP with ENDF/B-VI cross sections.

The experiments were also grouped according to the hydrogen to plutonium ratio and average energy of neutrons causing fission. The results are found in Tables 13 and 14 and plotted in Figures 4 and 5, respectively. For the H to Pu ratio, groupings were based on a per integer basis. For instance, cases that had hydrogen to plutonium ratios of 5.1, 5.2, 5.9, and 5.9 were grouped together with an average ratio of 5.5. For the average energy, the experiments were grouped as follows: E<20 MeV, 20<E<100 MeV, 100<E<200 Mev, 200<E<300 MeV, E>300 MeV. A bias was calculated for each group and is listed in the table and shown in the chart using the average of the average energy. Again, Case 17 is not included in either comparison. For both the H to Pu ratio and average energy grouping, the Δk_{avg} values are within the uncertainty of the bias values, in general. Again, the bias calculated using MCNP with ENDF/B-VI cross sections have lower absolute values of Δk_{avg} and a smaller spread than do the bias using the other two codes/cross section libraries.

Finally, bias values were calculated for all experiments as a single group. For MCNP with ENDF/B-V cross sections, the bias was 0.0020 ± 0.0037 (0.0008). For MCNP with ENDF/B-VI cross sections, the bias was 0.0005 ± 0.0035 (0.0008). The bias for KENO with ENDF/B-IV cross sections was found to be 0.0008 ± 0.0042 (0.0009). All of the values just given include Case 17. Excluding this experiment, the bias values were 0.0013 ± 0.0023 (0.0008) for MCNP with ENDF/B-V, -0.0003 ± 0.0020 (0.0008) for MCNP with ENDF/B-VI, and 0.0002 ± 0.0037 (0.0009) for KENO. As mentionned previously, exclusion of Case 17 from the bias calculation decreases the Δk_{avg} values and the spread for all codes/cross section sets. KENO with ENDF/B-IV cross sections has the smallest absolute value of Δk_{avg} while MCNP with ENDF/B-V has the largest. However, KENO has the largest spread about the average calculated k. ENDF/B-VI is the only code/cross section set that has a negative Δk_{avg} value. This implies that this code slightly underestimates k_{eff} for these types of experiments.

Table 10. Bias Values Based on Plutonium Mass Grouping.

Array Size (# exps)	Pu mass per array (g)	MCNP with ENDF/B-V	MCNP with ENDF/B-VI	KENO-V.a with ENDF/B-IV
2x2x2 (10)	24,231	0.0017 ± 0.0015 (0.0013)	-0.0004 ± 0.0017 (0.0013)	-0.0002 ± 0.0032 (0.0014)
2x2x3 (3)	36,309	-0.0022 ± 0.0013 (0.0021)	-0.0026 ± 0.0012 (0.0021)	-0.0046 ± 0.0035 (0.0023)
2x2x4 (2)	48,422	0.0036 ± 0.0002 (0.0024)	0.0016 ± 0.0025 (0.0024)	0.0043 ± 0.0001 (0.0026)
2x2x5 (1)	60,541	0.0051 ± [b] (0.0040)	0.0030 ± [b] (0.0040)	0.0048 ± [b] (0.0042)
3x3x3 (6)	81,764	0.0037 ± 0.0061 (0.0015)	0.0025 ± 0.0057 (0.0015)	0.0032 ± 0.0045 (0.0016)
3x3x3 [a] (5)	81,764	0.0007 ± 0.0017 (0.0013)	-0.0001 ± 0.0012 (0.0013)	0.0010 ± 0.0024 (0.0014)

[a] Case 17 not included.
[b] No spread for this group since there is only one experiment in that group.

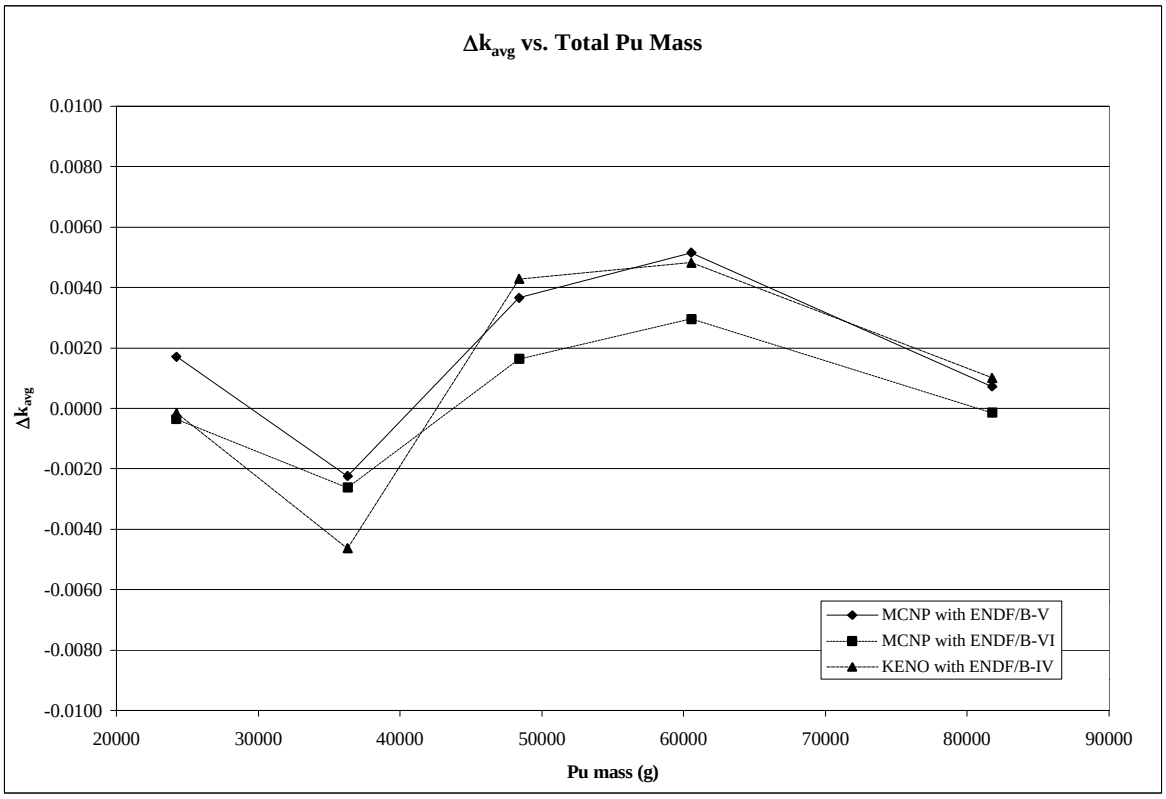

Figure 1. Δk_{avg} versus total plutonium mass. Plot does not include Case 17.

Table 11. Bias Values Based on Horizontal Spacing Grouping.

Horizontal Spacing (mm)	# of exp. in group	MCNP with ENDF/B-V	MCNP with ENDF/B-VI	KENO-V.a with ENDF/B-IV
76	5	0.0007 ± 0.0029 (0.0019)	-0.0006 ± 0.0028 (0.0019)	-0.0030 ± 0.0050 (0.0020)
90	3	0.0005 ± 0.0022 (0.0023)	-0.0010 ± 0.0003 (0.0014)	0.0001 ± 0.0009 (0.0015)
100	4	0.0020 ± 0.0015 (0.0018)	0.0004 ± 0.0024 (0.0018)	0.0012 ± 0.0022 (0.0019)
120	3	0.0064 ± 0.0087 (0.0021)	0.0049 ± 0.0082 (0.0021)	0.0037 ± 0.0075 (0.0023)
120 [(a)]	2	0.0006 ± 0.0031 (0.0023)	-0.0006 ± 0.0019 (0.0023)	-0.0010 ± 0.0051 (0.0026)
128.9 [(b)]	5	0.0009 ± 0.0018 (0.0015)	-0.0002 ± 0.0013 (0.0015)	0.0012 ± 0.0027 (0.0017)
141	1	0.0038 ± [(c)] (0.0034)	-0.0001 ± [(c)] (0.0034)	0.0043 ± [(c)] (0.0037)
170	1	0.0051 ± [(c)] (0.0040)	0.0030 ± [(c)] (0.0040)	0.0048 ± [(c)] (0.0042)

[(a)] case 17 not included
[(b)] horizontal spacing is average over five experiments with horizontal spacing between 127 and 130.5 mm.
[(c)] No spread for this group since there is only one experiment in that group.

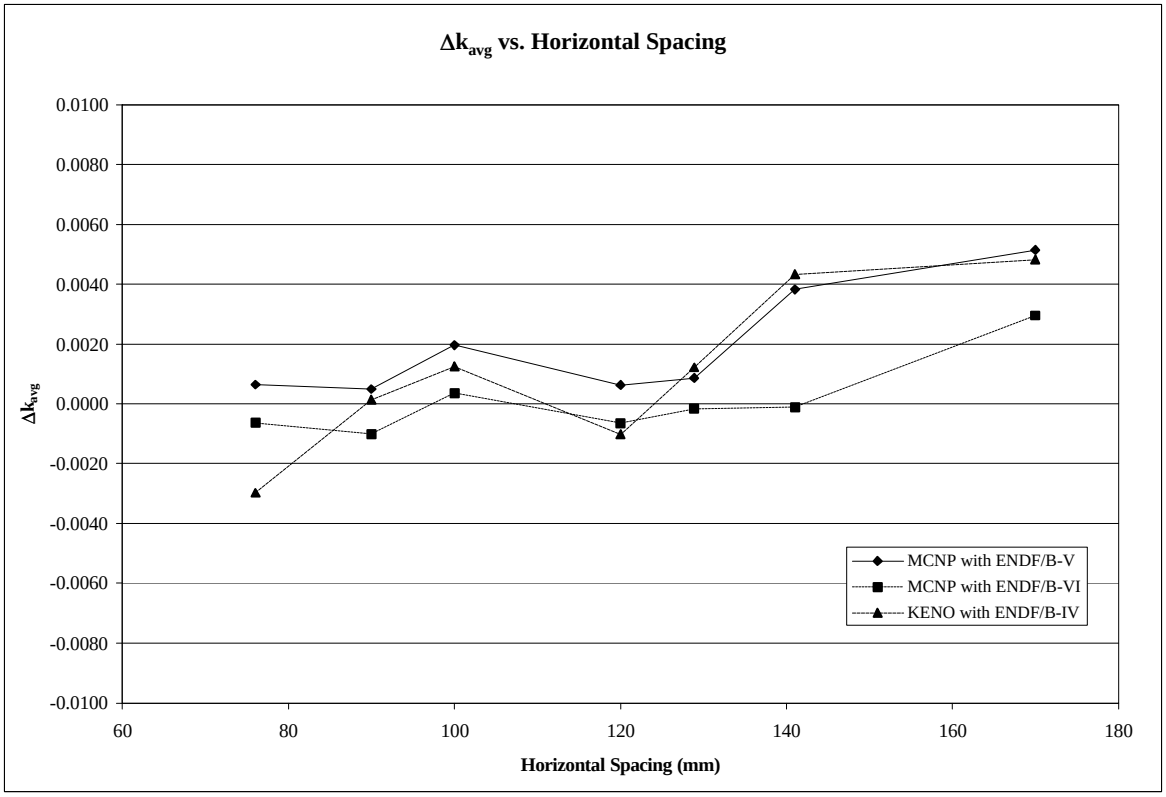

Figure 2. Δk_{avg} versus horizontal spacing. Plot does not include Case 17. Point at 128.9 mm is average of five experiments with horizontal spacings between 127 and 130.5 mm.

Table 12. Bias Values Based on Vertical Spacing Grouping.

Vertical Spacing (cm) [a]	# of exp. in group	MCNP with ENDF/B-V	MCNP with ENDF/B-VI	KENO-V.a with ENDF/B-IV
8.255	2	0.0040 ± 0.0017 (0.0026)	0.0018 ± 0.0016 (0.0026)	0.0037 ± 0.0016 (0.0028)
9.525	1	0.0038 ± [b] (0.0034)	-0.0001 ± [b] (0.0034)	0.0043 ± [b] (0.0037)
10.427	2	0.0029 ± 0.0001 (0.0027)	-0.0010 ± 0.0004 (0.0027)	0.0012 ± 0.0019 (0.0029)
11.815	1	-0.0015 ± [b] (0.0031)	-0.0020 ± [b] (0.0031)	-0.0046 ± [b] (0.0034)
12.737	6	0.0006 ± 0.0016 (0.0014)	-0.0005 ± 0.0014 (0.0014)	0.0008 ± 0.0026 (0.0015)
13.257	3	0.0020 ± 0.0018 (0.0023)	0.0006 ± 0.0024 (0.0023)	0.0005 ± 0.0006 (0.0024)
15.365	1	0.0035 ± [b] (0.0033)	0.0034 ± [b] (0.0033)	0.0042 ± [b] (0.0036)
17.395	1	-0.0015 ± [b] (0.0041)	-0.0019 ± [b] (0.0041)	-0.0012 ± [b] (0.0044)
18.415	1	0.0008 ± [b] (0.0045)	0.0000 ± [b] (0.0045)	-0.0053 ± [b] (0.0047)
21.465	1	-0.0004 ± [b] (0.0044)	-0.0029 ± [b] (0.0044)	-0.0057 ± [b] (0.0046)
23.495	1	0.0030 ± [b] (0.0044)	0.0010 ± [b] (0.0044)	0.0044 ± [b] (0.0046)
38.735	1	-0.0037 ± [b] (0.0039)	-0.0040 ± [b] (0.0039)	-0.0081 ± [b] (0.0042)

[a] Vertical spacing is average of spacing for group. Grouping based on a per centimeter basis. Case 17 is not included in these values.
[b] No spread for this group since there is only one experiment in that group.

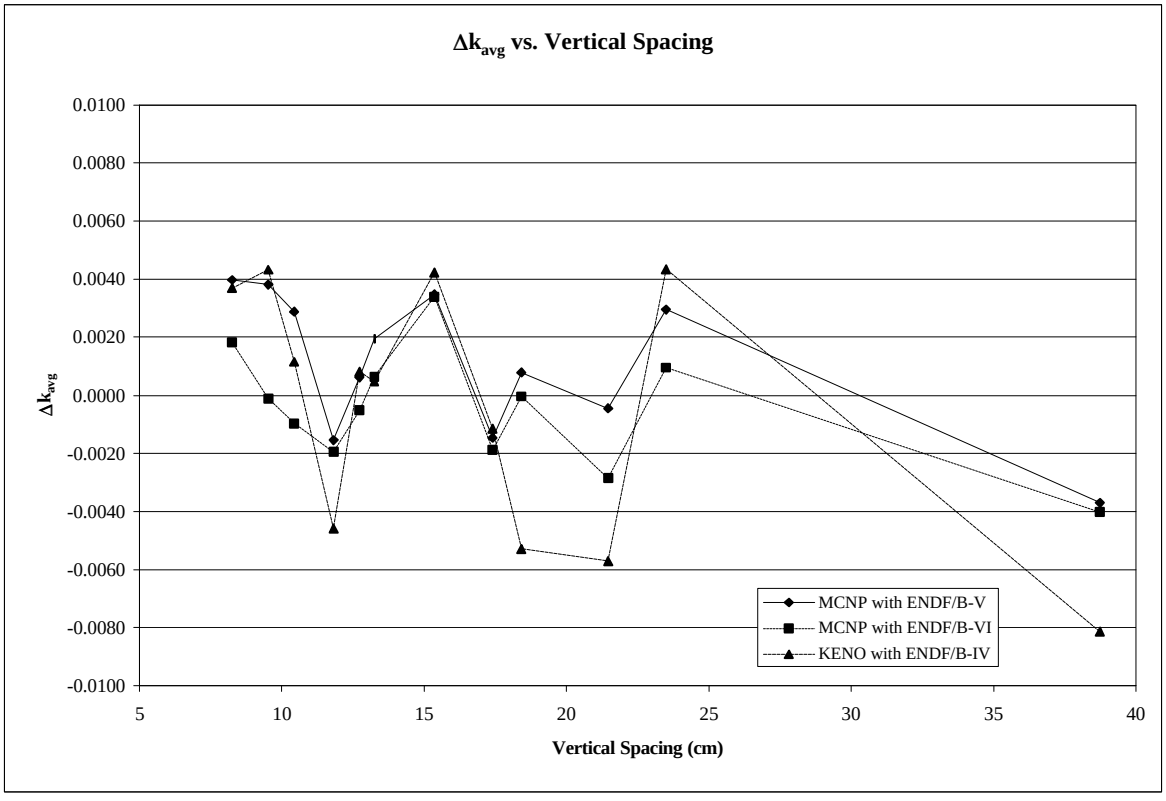

Figure 3. Δk_{avg} versus vertical spacing. Plot does not include Case 17. Experiments are grouped per centimeter.

Table 13. Bias Values Based on Hydrogen to Plutonium Ratio Grouping.

H to Pu Ratio [a]	# of exp. in group	MCNP with ENDF/B-V	MCNP with ENDF/B-VI	KENO-V.a with ENDF/B-IV
5.5	4	0.0022 ± 0.0040 (0.0020)	0.0004 ± 0.0033 (0.0020)	0.0002 ± 0.0060 (0.0021)
6.9	1	0.0030 ± [b] (0.0038)	-0.0012 ± [b] (0.0038)	0.0014 ± [b] (0.0041)
7.4	8	0.0009 ± 0.0017 (0.0013)	-0.0006 ± 0.0014 (0.0013)	-0.0005 ± 0.0037 (0.0014)
8.7	2	0.0006 ± 0.0031 (0.0023)	-0.0006 ± 0.0019 (0.0023)	-0.0010 ± 0.0051 (0.0026)
9	1	0.0000 ± [b] (0.0041)	-0.0020 ± [b] (0.0041)	0.0005 ± [b] (0.0043)
10.1	3	0.0017 ± 0.0017 (0.0020)	0.0007 ± 0.0027 (0.0020)	0.0013 ± 0.0027 (0.0022)
12.2	1	-0.0015 ± [b] (0.0041)	-0.0019 ± [b] (0.0041)	-0.0012 ± [b] (0.0044)
13.8	1	0.0030 ± [b] (0.0044)	0.0010 ± [b] (0.0044)	0.0044 ± [b] (0.0046)

[a] Ratio is average for group. Grouping based on a per integer basis (e.g. Cases that had H to Pu ratios of 5.1, 5.2, 5.9, and 5.9 were grouped together and appear in the table as H to Pu ratio of 5.5). Case 17 is not included in these values.
[b] No spread for this group since there is only one experiment in that group.

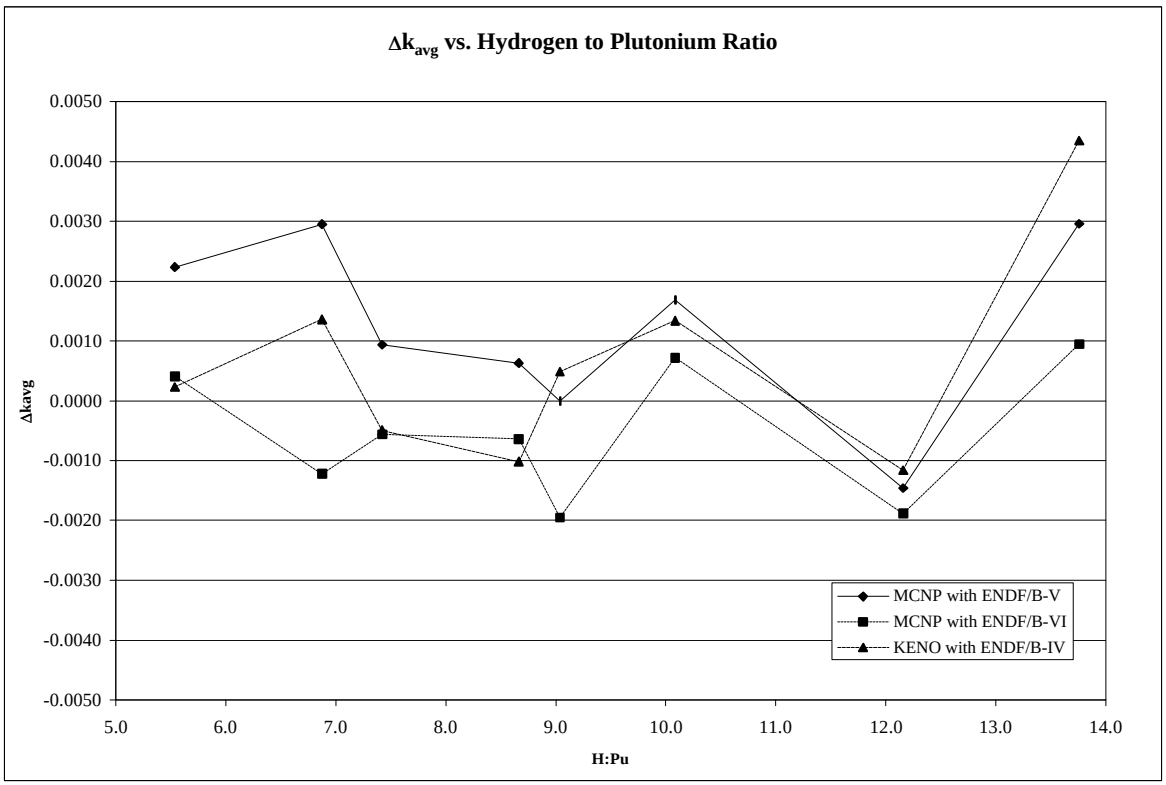

Figure 4. Δk_{avg} versus hydrogen to plutonium ratio. Plot does not include Case 17. Experiments are grouped as described in text and table.

Table 14. Bias Values Based on Average Energy of Neutrons Causing Fission.

Energy (MeV)[a]	# of exp. in group	MCNP with ENDF/B-V	MCNP with ENDF/B-VI	KENO-V.a with ENDF/B-IV
7	10	0.0011 ± 0.0019 (0.0010)	-0.0001 ± 0.0017 (0.0010)	0.0009 ± 0.0029 (0.0011)
36	5	0.0019 ± 0.0026 (0.0017)	-0.0002 ± 0.0021 (0.0017)	0.0015 ± 0.0023 (0.0019)
141	2	0.0030 ± 0.0000 (0.0029)	-0.0001 ± 0.0015 (0.0029)	0.0029 ± 0.0021 (0.0031)
217	3	-0.0011 ± 0.0023 (0.0025)	-0.0023 ± 0.0020 (0.0024)	-0.0064 ± 0.0015 (0.0026)
474	1	0.0037 ± [b] (0.0045)	0.0028 ± [b] (0.0045)	-0.0001 ± [b] (0.0047)

[a] Energy is the average energy of neutrons causing fission. The value listed is average of the average energy for group. Grouping is as follows: E<20 MeV, 20<E<100 MeV, 100<E<200 Mev, 200<E<300 MeV, E>300 MeV. Case 17 is not included in these values.
[b] No spread for this group since there is only one experiment in that group.

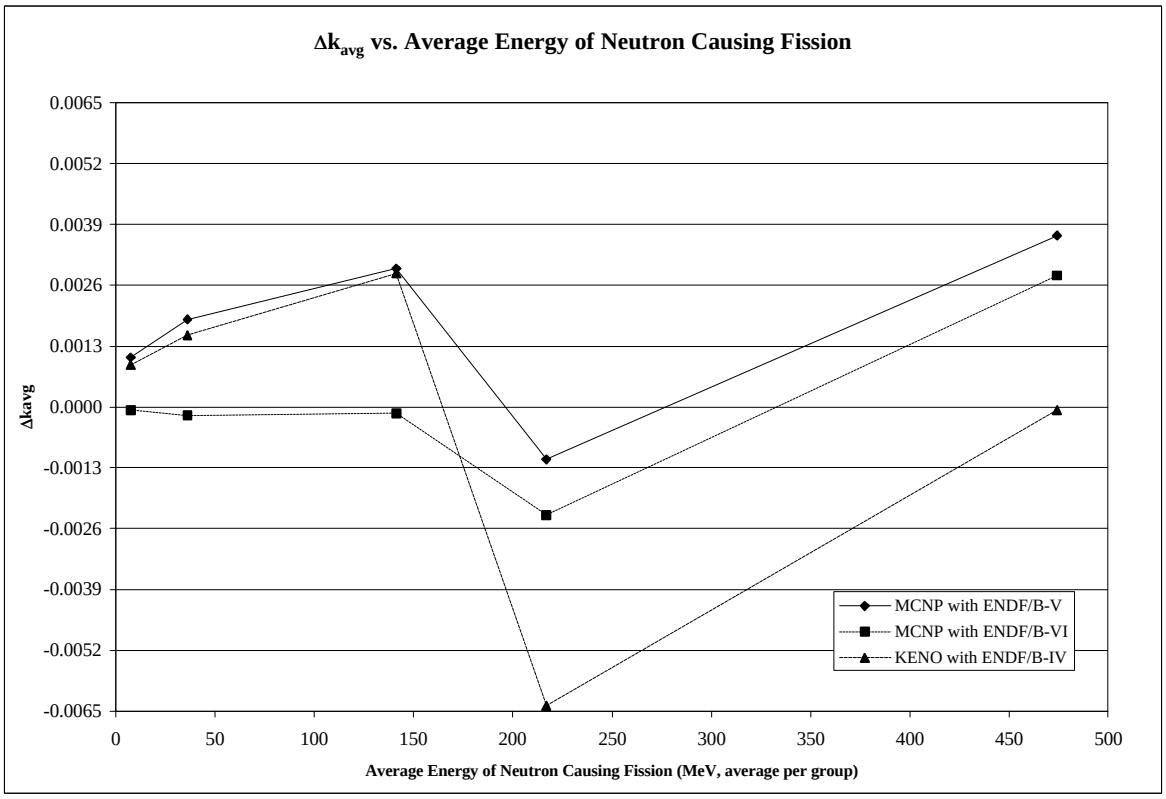

Figure 5. Δk_{avg} versus average energy of neutron causing fission. Plot does not include Case 17. Experiments are grouped as described in text and table.

V. Summary and Conclusions

Thirty-three experiments were analyzed as part of the International Criticality Benchmark Evaluation Project. These experiments were fully described in Part I of this paper. Of these, twenty-two were formed into benchmark models for validation of computer codes and cross sections. Repeated experiments were combined and formed a single benchmark model. Several other experiments described in Part I were not considered acceptable as benchmark experiments due to questionable data or large uncertainties in critical water height.

The benchmark models for the accepted experiments were derived in detail. Sixteen of the experiments were 2x2xN arrays of plutonium metal cylinders, where N ranged from 2 to 5. The remaining

six benchmark models were 3x3x3 arrays. All of the models used the same double-canned plutonium parts and were, at least, partially water-reflected. The geometry specifications and material atom densities were given for the benchmark models. Benchmark model k_{eff} values were found by correcting the experimental k_{eff}. The correction factor was the difference between the benchmark model and a fully detailed experiment model that included walls and room structures. Only one of the benchmark models had a statistically significant correction factor.

An uncertainty on the benchmark model k_{eff} value due to experiment uncertainties and omission of data from the benchmark model was found by sensitivity studies. Parameters that were analyzed include plutonium mass, plutonium density, plutonium dimensions, horizontal and vertical spacing, and critical water height.

Finally, a k_{eff} value was found for all benchmark models using MCNP with continuous energy ENDF/B-V cross section data, MCNP with continuous energy ENDF/B-VI cross section data, and KENO-V.a with 27-group ENDF/B-IV cross section data. For one experiment (Case 17), all codes/cross sections overestimated k_{eff} by more than 1%. Grouping the experiments according to three different parameters, bias values were found for all codes/cross section sets. No significant trend in the bias could be seen based on plutonium mass, horizontal spacing, vertical spacing, hydrogen to plutonium ratio, or average energy of neutrons causing fission. For the different parameters studied, MCNP with ENDF/B-VI cross sections had the smallest difference in the average k_{eff} (Δk_{avg}). Nonetheless, the smallest Δk_{avg} found for all experiments grouped together, excluding Case 17, was for KENO with ENDF/B-IV cross sections. However, MCNP with ENDF/B-VI had a comparable absolute value of the Δk_{avg} while having a significantly smaller spread than KENO. When Case 17 was not excluded, MCNP with ENDF/B-VI showed the smallest Δk_{avg}.

Acknowledgements

The information contained in this paper was developed in conjunction with the Westinghouse Savannah River Company during the course of work under contract number DE-AC09-96SR18500 serving with the U.S. Department of Energy.

References

1. R. Rothe, Experimental Critical Parameters of Plutonium Metal Cylinders Flooded with Water, INEL-96/0250, Idaho National Engineering Laboratory, 1996.
2. M. Pitts, F. Rahnema, and T.G. Williamson, “Flooded 2x2xN Arrays of 3-kg Plutonium Metal Cylinders – Phase 2,” PU-MET-FAST-037, NEA/NSC/DOC/(95)03/I, accepted 1998.
3. M. Pitts, F. Rahnema, and T.G. Williamson, “Flooded 3x3x3 Arrays of 3-kg Plutonium Metal Cylinders – Phase I,” PU-MET-FAST-016, NEA/NSC/DOC/(95)03/I, 1996.
4. J. F. Briesmeister, Ed., “MCNP-A General Monte Carlo Code for Neutrons, Photon, and Electorn Transport, Version 4A,” LA-12625-M, Los Alamos National Laboratory, 1986 (Rev. 1988 and 1991).
5. R. Kinsey, Ed., “ENDF/B Summary Documentation, 3rd Edition (ENDF/B-V),” BNL-NCS-17541 (ENDF-201), Brookhaven National Laboratory, 1979 (Revised 1980).
6. P. F. Rose, Ed., “ENDF/B Summary Documentation, 4th Edition (ENDF/B-VI),” BNL-NCS-17541 (ENDF-201), Brookhaven National Laboratory, 1991 (Release-2 1993).
7. “CCC-547 RSIC, SCALE 4.2: SCALE 4.2 Modular Code System for Performing Standardized Computer Analysis for Licensing Evaluations,” RSIC Computer Code Collection, CCC-545, Radiation Shielding Information Center.